Interference Analysis of Coexisting 5G Networks and NGSO FSS Receivers in the 12 GHz Band

Ta-seen Reaz Niloy, Zoheb Hassan, Nathan Stephenson, and Vijay K. Shah

***Abstract*—Despite the promising attributes of the 12 GHz band for expanding terrestrial 5G network's capacity and coverage, interference between coexisting networks remains a major issue. This paper develops a simulation-based evaluation framework and investigates the harmful interference between the 5G radio links and incumbent fixed non-geostationary satellite orbit (NGSO) fixed satellite services (FSS) receivers of the 12 GHz band. A variety of features including actual deployment locations of 5G base stations (BSs) and fixed NGSO FSS receivers, industry-standardized beamforming at BSs, directional signal reception at FSS receivers, realistic propagation channels with obstruction from buildings, and channel scheduling at 5G BSs are incorporated in the interference study. Simulation results conducted in a realistic urban-micro deployment scenario confirm that the terrestrial 5G networks with directional BSs can coexist in the 12GHz band by suitably selecting exclusion zone's radius around the FSS receiver. Simulation results also show that interference in the coexisting network can be notably reduced by appropriately activating BSs in the 12 GHz band based on their locations and surroundings.**

I. Introduction

With gigabyte-speed connectivity, enhanced reliability, and ultra-low latency, spectrum is the key commodity for terrestrial fifth-generation (5G) networks and beyond. Recently, the telecommunications industry and spectrum regulatory authorities are both increasingly interested in unlocking the 12 GHz band between $12.2 - 12.7$ GHz for two-way terrestrial 5G mobile services to address shortcomings of the existing sub-6 GHz and millimeter wave bands [1]. The 12 GHz band offers 500 MHz contiguous bandwidth for both uplink and downlink communications along with better propagation and building penetration capabilities than commercially deployed mmWave bands. However, interference between proposed 5G radio links and existing incumbents poses a key challenge in accommodating terrestrial 5G networks in the 12 GHz band. In USA, the 12 GHz band is currently licensed to three different services, namely, direct broadcast satellite service (DBS), non-geostationary orbit fixed satellite service (NGSO FSS), and multichannel video and data distribution service (MVDDS). The *harmful* interference from the coexisting 5G radio links can cause serious service degradation for these incumbent licenses. Hence, a realistic interference analysis framework is required to access the feasibility of coexistence of terrestrial 5G networks in the 12 GHz band.

In state-of-the-art literature, interference between the coexisting terrestrial cellular networks and incumbent receivers of S-band at $3.55 - 3.65$ GHz spectrum and C-band at $3.7 - 3.98$ GHz spectrum were extensively studied [2]–[5]. However, in comparison to both S and C bands, the 12 GHz band has different propagation characteristics and incumbents' features, including, antenna patterns, heights, and deployment strategies. Consequently, a clean-slate interference evaluation framework is required for the 12 GHz band. Recently, some industry-specific studies have been conducted, where [6], [7] investigated interference between terrestrial 5G and NGSO FSS networks in the 12 GHz band, and study [8] investigated interference between terrestrial 5G and DBS networks. These studies, [6], [7] however provided contradictory conclusions in terms of the coexistence scenario of 5G MBS and NGSO FSS receiver, where article [6] reported, in 99.85% of instances, the 5G MBS can coexist without interfering with the NGSO FSS receiver and [7] said, the 5G MBS can interfere with NGSO FSS receivers, degrading coverage by 77% in 12GHz band. At the same time, the assumptions used in these studies have certain limitations in path loss analysis. Specifically, the authors in [6] considered 3GPP probabilistic method and ignored site-specific local-factors for path loss analysis. Meanwhile, only randomly generated line-of-sight (LOS) and non-line-of-sight (NLOS) interference links were considered in [7]. However, realizations of the LOS and NLOS paths in practice can be vastly different from the probability model-based predictions. We emphasize that the probabilistic method can severely underestimate or overestimate the path loss and resultant interference [9], [10]. For instance, the authors of [10] compared the exact channel models that are developed for the 13 GHz band through experiments and concluded that the path loss provided by the 3GPP model notably deviates from the exact channel model. Although a similar type of experiment for the 12GHz band is not available, we expect the result would be the same for the 12 GHz band. Furthermore, the studies conducted by industrial licenses considered random deployment scenarios for 5G MBS without considering the exclusion zone's radius and strategies to protect FSS receiver from harmful interference. Accordingly, the motivation behind this study is two fold: first, to create a flexible and realistic interference analysis framework for the 12 GHz band, and second, to demonstrate the framework's effectiveness in developing context-aware policies to mitigate harmful interference in practical deployment scenarios.

In this work, we develop a realistic simulation-based interference evaluation framework for the 12 GHz band. Different from the existing literature, the developed framework incorporates the following novel attributes. Firstly, the actual deployment information of terrestrial 5G MBSs and FSS receivers are incorporated. Secondly, a realistic propagation environment is developed by leveraging real information about buildings along with a method for estimating path loss from coexisting MBSs to the FSS receiver. Thirdly, a variety of features including

T. R. Niloy, N. Stephenson, and V. K. Shah are with NextG Wireless Lab, George Mason University, VA, USA. Z. Hassan is with Virginia Tech, VA, USA. (Corresponding author's e-mail: tniloy@gmu.edu). This work was supported by NSF grants CNS-2128540 and CNS-2128584.

This article has been accepted for publication in IEEE Wireless Communications Letters. This is the author's version which has not been fully edited and content may change prior to final publication. Citation information: DOI 10.1109/LWC.2023.3281769

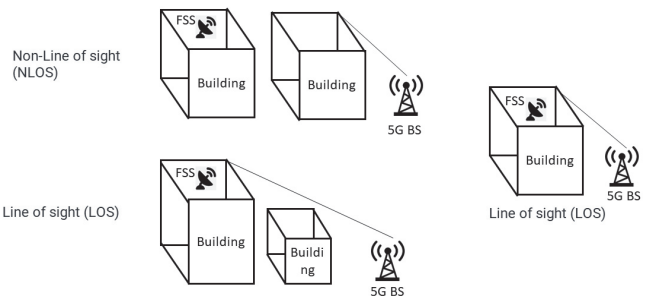

Fig. 1: Visual Representation of LOS and NLOS Links from interfering MBS to FSS receiver.

industry-standardized beamforming at MBSs, directional signal reception at FSS receivers, and channel scheduling at 5G MBSs are also integrated. We emphasize that this is the first study to develop an open-source interference simulator for spectrum coexistence between terrestrial 5G and incumbents in the 12 GHz band. A case study representing an urban-micro deployment scenario in Blacksburg, Virginia, USA is simulated to study interference from terrestrial 5G macro BSs (MBSs) to the FSS receiver. Several results are presented to reveal insights into the impact of beamforming at 5G BSs, exclusion zone's radius, and MBS activation criteria on the overall interference. We will release the developed simulator publicly to encourage further research in the 12 GHz band and reproduce results.

II. System Model

We consider a system of M 5G MBSs and an FSS receiver. To obtain an accurate estimation of the downlink interference from terrestrial 5G network to FSS receiver, we consider actual deployment locations of these MBSs obtained from the OpenCellID database [11]. In addition, MBSs are placed at a height that is appropriate for their deployment scenarios. As per 3GPP specifications, heights of MBSs are set at 35 meters for rural deployment scenarios, 25 meters for urban macro, and 10 meters for urban-micro. Each MBS is assumed to have a coverage over a circular area of radius R meter where the value of R depends on the deployment scenarios. Furthermore, the coverage region of each MBS is divided into three equal sectors of 120 degrees. The user equipments (UEs) are randomly dropped in the coverage region of each MBS. Each MBS operates in the $12.2 - 12.7$ GHz band, which is further segregated into a total of five 100 MHz channels. Without further specification, we consider that MBSs employ directional antennas. Specifically, similar to [6], [7], we consider that each MBS can support up to four UEs per channel using beamforming. Hence, each MBS can simultaneously support a maximum of 20 UEs per sector. The MBSs are considered to be 50% loaded, and thus, each MBS simultaneously transmits to a total of 30 UEs. We assume that MBSs know the accurate positions of the UEs located in their coverage region, and thereby, can form a directional beam towards each UE.

As for the deployment of FSS receiver, we consider an antenna height of 4.5 meters. This is practical since FSS receivers are typically installed on rooftops to get better signal coverage [7]. FSS receiver's pointing angle is set to an appropriate value to enhance strength of the signal received from the satellite transmitter. This is motivated by the fact that the co-channel interference from coexisting 5G networks can be kept to a small value for a wide range of pointing angles as long as the dynamic and static contexts of network are appropriately exploited by the terrestrial network operators. The FSS receiver operates in the $10.7 - 12.7$ GHz band. This band is divided into a total of eight 240 MHz bandwidth channels, each separated by a 10 MHz guard band. It is assumed that the FSS receiver can receive data from its satellite transmitter over one or more of these eight channels simultaneously [6].

III. Interference Analysis Framework

A. Required Components for Interference Analysis

1) Transmitter Antenna Gain of Interfering BS: Each 5G MBS is equipped with a $N_h \times N_v$ planner antenna array where N_h and N_v are the numbers of antenna elements in the row and column of the array. Each BS forms multiple beams, and we assume that each beam is directed to a particular UE. In accordance with the 3GPP antenna pattern, the overall antenna gain (in dBi unit) of the beam directed to the i-th UE at a particular azimuth angle $\phi_i \in [-\pi, \pi]$ and elevation angle $\theta_i \in [0, \pi]$ is obtained as [12]

$$G_{5G}^{(i)}(\theta_i, \phi_i) = A_E(\theta_i, \phi_i) + A_V(\theta_i, \phi_i) \tag{1}$$

where $A_E(\theta_i, \phi_i)$ and $A_V(\theta_i, \phi_i)$ are the antenna element gain and array gain in dBi unit, respectively. The antenna element gain is further expressed as

$$A_E(\theta_i, \phi_i) = G_{E,\max} - \min\left(-[(A_{E,V}(\theta_i) + A_{E,H}(\phi_i)], A_m\right) \tag{2}$$

where $G_{E,max}$ is the maximum gain of an antenna element, $A_{E,V}$ and $A_{E,H}$ are the vertical and horizontal radiation patterns, respectively, and A_m is the front-to-back ratio in the dB. The values of $G_{E,\max}$ and A_m are set to -8 dBi and 30 dB, respectively. Furthermore, the vertical and horizontal radiation patterns are expressed as

$$A_{E,H}(\phi_i) = -\min\left[12 \times (\phi_i/\phi_{3dB})^2, A_m\right], \tag{3}$$

and

$$A_{E,V}(\theta_i) = -\min\left[12 \times ((\theta_i - 90^\circ)/\theta_{3dB})^2, S_L\right] \tag{4}$$

where ϕ_{3dB}, θ_{3dB}, and S_L are vertical half-power beamwidth, horizontal half-power beamwidth, and side-lobe suppression level, respectively. As per 3GPP specification, we consider $\phi_{3dB} = 90^\circ$, $\theta_{3dB} = 65^\circ$, and $S_L = 30$ dB. The array gain is computed as

$$A_V(\theta_i, \phi_i) = 10\log_{10}(|\mathbf{V}^H(\theta_i, \phi_i)\mathbf{W}(\phi_{scan,i})|^2) \tag{5}$$

where $\mathbf{V}^H(\theta_i, \phi_i)$ and $\mathbf{W}(\phi_{scan,i})$ are $N_h \times N_v$-long steering and beamforming vectors, respectively, and $\phi_{scan,i}$ is the scanning angle. The (m, n)-th elements of $\mathbf{V}^H(\theta_i, \phi_i)$ and $\mathbf{W}(\phi_{scan,i})$ are expressed as

$$\begin{aligned} v_{m,n}(\theta_i, \phi_i) = \exp\Bigg(j2\pi\Bigg((m-1)\frac{d_v}{\lambda}\cos\theta_i \\ +(n-1)\frac{d_h}{\lambda}\sin\theta_i\sin\phi_i\Bigg)\Bigg), \end{aligned} \tag{6}$$

and

$$\begin{aligned} w_{m,n}(\phi_{scan,i}) = \frac{1}{\sqrt{MN}}\exp\Bigg(j2\pi\Bigg((m-1)\frac{d_v}{\lambda}\sin\theta_{tilt} \\ +(n-1)d_h\lambda\cos\theta_{tilt}\sin\phi_{scan,i})\Bigg), \end{aligned} \tag{7}$$

respectively. In (6) and (7), d_h and d_v denote the spacing between two antenna elements in the row and column of the antenna array, respectively; λ is the wavelength; θ_{tilt} and $\phi_{scan,i}$ are the downtilt and electrical scan angles, respectively. Note that θ_{tilt} is set to a fixed value in order to optimize the coverage of each MBS whereas $\phi_{scan,i} \in [-\pi, \pi]$ is optimally chosen to maximize the antenna gain at (θ_i, ϕ_i) direction.

2) Receiver Antenna Gain of FSS: Similar to the study from NGSO-FSS licensee [7], the Class B wide band earth stations communicating with non-geostationary satellite systems (WBES) antenna pattern, standardized by ETSI, is employed for the FSS receiver. For such an antenna pattern, the received gain at a certain angle ϕ from the boresight direction is modeled as

$$G_{FSS}(\phi) = \begin{cases} 40 - 25\log\phi \text{ dBi} & 6^\circ \leq \phi < 48^\circ \\ -2 \text{ dBi} & 48^\circ \leq \phi \leq 180^\circ. \end{cases} \tag{8}$$

3) Path Loss between Interfering BS and FSS: The path loss (in dB unit) from the m-th interfering MBS to FSS receiver is determined as [2, eq. (1)]

$$\begin{aligned} \text{PL}(d_m) = \mathbf{1}_{(\beta=0)} \left(\text{PL}_{\text{NLOS}}(d_m) + X(\sigma_{\text{NLOS}})\right) \\ + \mathbf{1}_{(\beta=1)} \left(\text{PL}_{\text{LOS}}(d_m) + X(\sigma_{\text{LOS}})\right) \end{aligned} \tag{9}$$

where $\beta \in \{0, 1\}$ such that $\beta = 0$ and $\beta = 1$ represent the NLOS and LOS propagation scenarios, respectively, and $\mathbf{1}_{(\cdot)}$ is an indicator function; d_m is the distance between the m-th MBS and FSS receiver; $\text{PL}_{\text{NLOS}}(d_m)$ and $\text{PL}_{\text{LOS}}(d_m)$ represent the path losses in dB for NLOS and LOS propagation scenarios; and $X(\sigma_{\text{k}})$ represents shadow fading loss in dB with σ_k as the standard deviation and $k \in \{\text{LOS, NLOS}\}$. In the existing literature of the 12 GHz band, the LOS and NLOS paths are determined using probabilistic models of [13, Table 7.4.2]. However, such probabilistic models primarily depend on the distance between MBS and user terminals. In practice, the realizations of LOS and NLOS paths depend on a number of factors, including the building's shapes and heights, heights of incumbent receivers, and weather-specific effects such as scattering due to precipitation. Motivated by this fact, we propose a computationally efficient method to obtain accurate LOS and NLOS propagation paths. In particular, by leveraging OpenStreetMap[1], we first integrate information of the positions, heights, and shapes of all the buildings in the considered region. Subsequently, by using certain geometric manipulations, we determine whether the interference axis from an MBS to FSS receiver intersects with a building polygon or not. The link between an MBS and FSS receiver is LOS if there is no obstruction in the interference axis, and NLOS otherwise. The overall procedure is depicted in Fig. 1, We utilize the 3GPP path loss models, defined in [13, Table 7.4.1], to determine the values of $\text{PL}_{\text{NLOS}}(d_m)$ and $\text{PL}_{\text{LOS}}(d_m)$. This is because (i) there are no unified path loss models proposed for the 12 GHz band and (ii) the path loss models proposed by 3GPP are standardized for $0.5 - 100$ GHz frequency range. Note that the values of $\text{PL}_{\text{NLOS}}(d_m)$ and $\text{PL}_{\text{LOS}}(d_m)$ vary in different deployment contexts. In the simulator, we implement the population density per square mile threshold rule, proposed by [6], to classify a given region into urban-macro, urban-micro, and rural deployment contexts, and determine the path loss accordingly. We emphasize that the considered geometric method is generic and can incorporate any appropriate path loss models for the 12 GHz band.

4) Set of Interfering Beams from 5G MBS: As evident from the previous discussion, the terrestrial 5G and FSS operations overlap in the $12.2 - 12.7$ GHz band. In this band, FSS receiver uses two different channels with frequency ranges from $12.2 - 12.45$ GHz and $12.45 - 12.7$ GHz, denoted by FSS-CH-1 and FSS-CH-2, respectively. Meanwhile, the $12.2 - 12.7$ GHz band for downlink MBS operation is divided into the following five 100 MHz channels: (i) MBS-CH-1 ($12.2 - 12.3$ GHz), (ii) MBS-CH-2 ($12.3 - 12.4$ GHz), (iii) MBS-CH-3 ($12.4 - 12.5$ GHz), (iv) MBS-CH-4 ($12.5 - 12.6$ GHz) and (iv) MBS-CH-5 ($12.6 - 12.7$ GHz). Note that the scheduling of UEs in these channels determines the set of interfering beams transmitted from an MBS. As mentioned in Section III, an MBS transmits a single directional beam to each UE of its coverage. Accordingly, depending on the channel usage pattern of FSS, either the entire or only a partial set of the transmitted beams can interfere with FSS receiver. We denote $\mathcal{U}$ as the total set of UEs under the coverage of the m-th MBS. Moreover, $\mathcal{U} = \mathcal{U}_1 \cup \mathcal{U}_2$ where $\mathcal{U}_1$ represents the set UEs scheduled in the MBS-CH-1, MBS-CH-2, and MBH-CH-3, and $\mathcal{U}_2$ represents the set UEs scheduled in the MBS-CH-3, MBS-CH-4, and MBH-CH-5. Therefore, the set of interfering beams transmitted from the m-th MBS, denoted by $\mathcal{U}_m$, is obtained as

$$\mathcal{U}_m = \begin{cases} \mathcal{U}, & \text{Both FSS-CH-1 and FSS-CH-2 are active} \\ \mathcal{U}_1, & \text{Only FSS-CH-1 is active} \\ \mathcal{U}_2, & \text{Only FSS-CH-2 is active} \end{cases} \tag{10}$$

Recall, an MBS can transmit a maximum of four beams to four different UEs per 100 MHz downlink channel in each sector. To satisfy this constraint, we first randomly assign UEs of a particular MBS's coverage to different downlink channels as such no downlink channel is occupied by more than four UEs. Thereafter, we apply (10) to determine the set of interfering beams for each MBS. Note that in the simulations, we consider random UE-downlink MBS channel scheduling for simplicity. However, the aforementioned methodology is applicable to any scheduling mechanism.

B. Aggregated Interference Evaluation:

We consider that the total power of each MBS is equally divided among all the transmitted beams. Here, total power (P_t) of each MBS in Watt, and a total of $|\mathcal{U}|$ UEs are covered by each BS. Therefore, the power (in dB unit) directed to the i-th UE of the m-th MBS is obtained as $P_{i,m} = 10\log_{10} P_t - 10\log_{10}|\mathcal{U}|$. The azimuth and elevation angles between the beam directed to the i-th UE and interference axis from the m-th MBS to FSS receiver are denoted by $\hat{\theta}_{i,m}$ and $\hat{\phi}_{i,m}$, respectively. Moreover, he angle between the FSS receiver's boresight and interference axis from the m-th MBS is denoted by $\tilde{\phi}_{m,FSS}$. The received interference (in dB unit) at the FSS receiver caused by the i-th transmitted beam from the m-th MBS is expressed as

$$I_m^{(i)} = P_{i,m} + G_{5\text{G}}^{(i)}(\hat{\theta}_{i,m}, \hat{\phi}_{i,m}) + G_{FSS}(\tilde{\phi}_{m,FSS}) - \text{PL}(d_m). \tag{11}$$

By leveraging (10), we obtain the set of interfering beams transmitted from m-th MBS. Hence, the total interference (in Watt) caused by the m-th MBS is expressed as $I_m = \sum_{i \in \mathcal{U}_m} 10^{\frac{I_m^{(i)}}{10}}$.

[1]OpenStreetMap is a public database of the buildings' information [14].

This article has been accepted for publication in IEEE Wireless Communications Letters. This is the author's version which has not been fully edited and content may change prior to final publication. Citation information: DOI 10.1109/LWC.2023.3281769

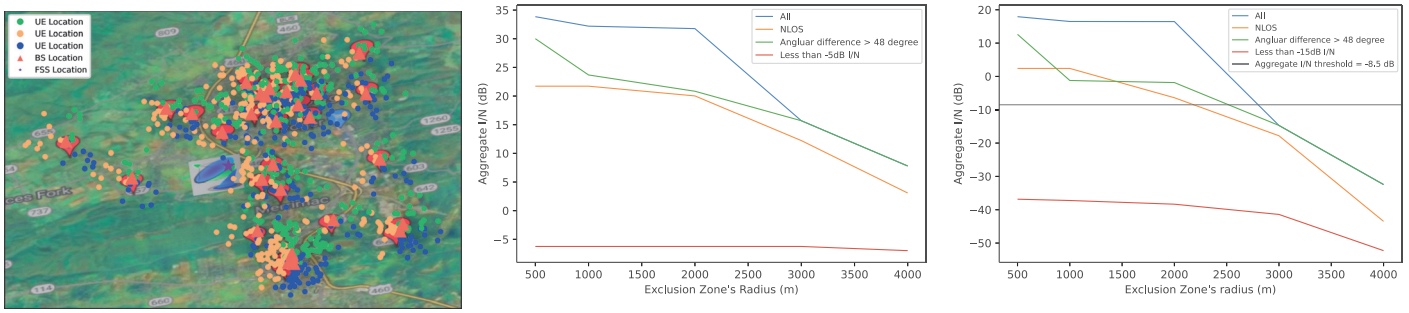

(a) (b) (c)

Fig. 2: (a) Simulation Setting with FSS, MBS, and UEs, (b) Aggregate I/N ratio vs exclusion zone's radius for omnidirectional MBSs, and (c) Aggregate I/N ratio vs exclusion zone's radius for directional MBSs.

Finally, the aggregate interference-to-noise (I/N) ratio (in dB) at the FSS receiver is obtained as

$$I/N = 10\log_{10}\left(\sum_{m=1}^{M} I_m\right) - 10\log_{10}\left(kTB\right) \qquad (12)$$

where k, T, and B are respectively the Boltzman constant, noise temperature, and bandwidth of the FSS receiver, respectively.

IV. Simulation Results and Discussions

a) Simulation Setup: For simulations, we consider the coexistence of terrestrial downlink 5G MBS and FSS at the 12 GHz band in Blacksburg, Virginia, USA. The population density of Blacksburg Town is 2,270 per square mile [15], and consequently, in accordance with [6], the deployment context belongs to sub-urban category. The FSS receiver is located at 1770 Forecast Drive, Blacksburg, Virginia, and its latitude and longitude are obtained as 37 12'9" North and 80 26' 4" West, respectively. A circular area of 5000 meter (m) radius is constructed by placing the FSS receiver in the center position. Using OpenCellID, a database of the existing cellular towers of Blacksburg Town is obtained, and from that database, a total of 33 global mobile systems (GSM) MBSs are found within a 5000m radius of the FSS receiver. For each MBS, a 1000m cellular coverage area is considered with three 120° sectors and 10 randomly deployed UEs at each sector. Furthermore, a geolocation dataset for the building blocks of Blacksburg Town, collected from OpenStreetMap by using overpass-turbo, is integrated into the simulator. A total of 8644 building information is acquired from the dataset about heights, physical coordinates, and shapes of the buildings. The minimum and maximum heights of the buildings are 10m and 40m, respectively. For each MBS, in addition to the parameters specified in Sections II and III, we consider (i) 16×16 antenna array with 0.5λ inter-antenna element spacing at both horizontal and vertical directions; (ii) 10° downtilt angles; and (iii) $P_t = 38$ dBm/100 MHz transmit power limit. Meanwhile, we consider that the pointing angle and noise temperature of the FSS receiver are 15° and 200 K, respectively. A representative system deployment scenario is depicted in Fig. 2a, where the locations of the FSS, MBSs, and UEs are shown based on their actual geographic coordinates.

b) Interference analysis for individual MBS: Fig. 3 shows the statistical variation of I/N ratio from individual MBS. We conduct the simulation experiment several times by randomly varying the UE locations and scheduling these UEs to available MBS downlink channels. Thus, in every simulation experiment, the interfering beams from each MBS vary, resulting in a variation in total interference power at the FSS receiver. In Fig. 3, we use boxplots to illustrate interference variation. It is observed that changing positions or scheduling of UEs cause around 2 to 5 dB variation of interference from a particular MBS. The interference behavior of a particular MBS is, however, influenced by its position and surroundings. It is evident in Fig. 3 that some MBSs introduce severe interference to the FSS receiver despite their large distances. Since the LOS link has a much smaller path loss than the NLOS link, an MBS that has a direct LOS link can generate much greater interference to the FSS receiver than its neighboring NLOS MBSs. An MBS can also create strong interference at the FSS receiver when its interference axis is aligned with the boresight direction of the FSS receiver. Note that the interference axis represents the direction of receiving interference from an MBS. If such a direction is varied from the furthest side lobe within the antenna main lobe, using (11), we can easily justify that the received interference varies by around 20 dB for a singly interfering beam. Hence, MBSs can generate a large I/N ratio at the FSS receiver as long as they have direct LOS links to the FSS receiver and have a small angular difference between their interference axis and FSS receiver's boresight direction. Overall, the deployment contexts of terrestrial 5G MBSs, namely, positions, distances from incumbents, and surrounding environment must be carefully considered for coexistence in the 12 GHz band.

c) Interference Analysis for Various Exclusion Zone's Radius: Figs. 2b and 2c illustrate aggregate I/N ratios for omnidirectional and directional MBSs with different exclusion zone's radius, respectively. An exclusion zone is a circular area around the FSS receiver such that only the MBSs outside the exclusion zone are able to transmit simultaneously in the 12 GHz band. There is a trade-off between protecting FSS receivers from harmful interference and maximizing the use of the 12 GHz band in terrestrial 5G networks, as increasing the radius of the exclusion zone leads to a decrease in the number of active MBSs and aggregate I/N ratio. To identify active MBSs outside the exclusion zone, we consider the following criteria.

1) **Criterion I (All):** All the MBSs outside the exclusion zone are allowed to transmit in the 12 GHz band.
2) **Criterion II (NLOS):** The MBSs that are outside the exclusion zone and have only NLOS links with the FSS are allowed to transmit in the 12 GHz band.

This article has been accepted for publication in IEEE Wireless Communications Letters. This is the author's version which has not been fully edited and content may change prior to final publication. Citation information: DOI 10.1109/LWC.2023.3281769

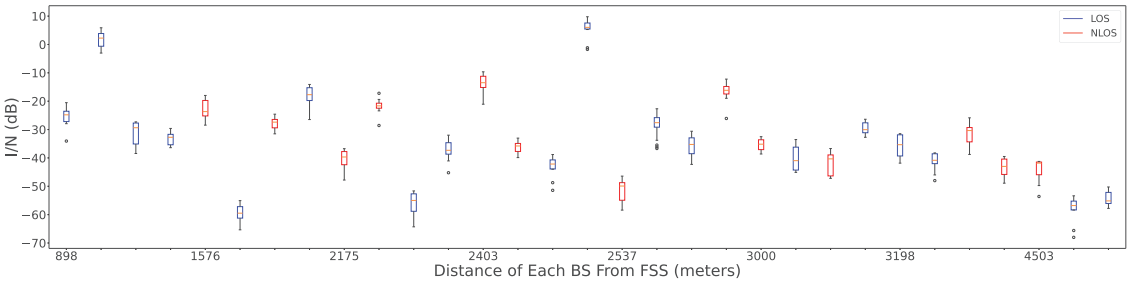

Fig. 3: Boxplot of I/N ratio from individual MBS versus (vs.) distance.

3) **Criterion III (Angular difference $>$ 48 degree):** The MBSs that are outside the exclusion zone and whose interference axis is at least $48°$ away from the boresight direction of the FSS antenna are allowed to transmit in the 12 GHz band.
4) **Criterion IV (Less than -5 dB I/N):** The MBSs that are outside the exclusion zone and do not generate an I/N ratio more than a certain threshold are allowed to transmit in the 12 GHz band. The threshold I/N ratio is -5 dB and -15 dB for omnidirectional and directional MBSs, respectively.

We consider a threshold aggregate I/N ratio of -8.5 dB for spectrum coexistence between terrestrial 5G and FSS [6], [7]. Figs. 2b and 2c depict that directional MBSs cause less interference than omnidirectional MBSs. In particular, the omnidirectional MBSs cannot achieve an aggregate I/N ratio lower than -7 dB, 1.5 dB higher than the I/N ratio necessary for spectrum coexistence. Because of broadcasting, an omnidirectional MBS causes interference to the FSS receiver from all directions. A directional MBS, in contrast, only transmits power in a few specific directions, and therefore the FSS receiver receives only a fraction of the total transmitted power. Fig. 2c shows that with directional MBSs, the aggregate I/N ratio can be reduced up to -38 dB, i.e., the beamforming capability of MBSs can provide a significant 31 dB interference reduction in the coexistence scenarios. Consequently, directional MBSs play a critical role in reducing co-channel interference to the FSS receiver.

Note that criterion I is a conventional context-agnostic policy that turns on and off any BSs that are outside and inside of the considered exclusion zone, respectively, without considering any contextual information. Meanwhile, criteria II to IV provide various site-specific context-aware policies for turning on/off BSs. Fig. 2c shows that the MBSs activated using criteria II-IV always achieve the lowest aggregate I/N ratios in comparison to criterion I, indicating a clear advantage of context-aware BS turning on/off policies. More specifically, by selecting a suitable policy, one can simultaneously activate a high number of MBSs in the 12 GHz band without generating harmful interference at the FSS receiver, thereby improving the utilization of the 12 GHz band. From Fig. 2c, we can see that the minimum required radius for exclusion zones to achieve an aggregate I/N ≤ -8.5 dB for criteria I, II, III, and IV is approximately 3000m, 2500m, 2000m, and 500m, respectively. Because criterion IV has a smaller exclusion zone, it can activate more MBSs in the 12 GHz band. Using Table I, we find that the maximum numbers of MBSs activated by criteria I, II, III, and IV are 11, 11, 25, and 29, respectively to achieve the threshold value. More precisely, compared to context-agnostic policy, criterion IV can improve the utilization of the 12 GHz band for the considered simulation scenario by 2.63 times. Accordingly, site-specific deployment contexts of the MBSs play a critical role in reducing co-channel interference to the FSS receiver.

TABLE I: # active directional MBSs outside exclusion zone

Exclusion zone's radius	Criteria I	Criteria II	Criteria III	Criteria IV
500m	33	13	33	29
1000m	31	13	31	28
2000m	25	11	25	23
3000m	11	5	11	11
4000m	3	1	3	3

V. Conclusion

A realistic interference evaluation framework is developed to study interference in terrestrial 5G-FSS coexistence in the 12 GHz band. Simulation results showed that directional MBSs more efficiently reduce the overall I/N ratio at FSS receivers than omnidirectional MBSs. In addition, we proposed four different MBS activation criteria to address the inherent trade-off between reducing harmful interference at the FSS receiver and increasing the number of active MBSs in the 12 GHz band. The simulation results indicated that by activating directional MBSs according to criterion IV outside a 500m radius exclusion zone, a significantly small aggregate I/N ratio is obtained.

References

[1] Z. Hassan *et al.*, "Spectrum sharing of the 12 GHz band with two-way terrestrial 5G mobile services: Motivations, challenges, and research road map," *IEEE Commun. Mag.* (early access).
[2] G. Hattab *et al.*, "Interference analysis of the coexistence of 5G cellular networks with satellite earth stations in 3.7-4.2 GHz," *IEEE International Conference on Communications Workshops*, 2018 pp. 1–6.
[3] Y. Wei *et al.*, "Distance protection for coexistence of 5g base station and satellite earth station," *Electronics*, vol. 10, no. 12, 2021.
[4] Saha *et al.*, "Spectrum sharing in satellite-mobile multisystem using 3D inbuilding small cells for high spectral and energy efficiencies in 5G and beyond era," *IEEE Access*, vol. 7, pp. 43846–43868, 2019.
[5] S. Bhattarai *et al.*, "Defining incumbent protection zones on the fly: Dynamic boundaries for spectrum sharing," *IEEE International Symposium on Dynamic Spectrum Access Networks (DySPAN)*, 2015, pp. 1–12.
[6] RKF Eng. Solutions, "Assessment of feasibility of coexistence between NGSO FSS earth stations and 5G operations in the 12.2–12.7 GHz band," Tech. Rep., May 2021.
[7] SpaceX, "Spacex analysis of the effect of terrestrial mobile deployment on NGSO FSS downlink operations, " Tech. Rep., June. 2022.
[8] DIRECTV, "12 GHz co-frequency interference from terrestrial mobile into DBS," Tech. Rep., July. 2022.
[9] N. Y. Mitsuishi *et al.*, "Path Loss Characterization of 7-GHz Terrestrial Propagation Channel in Urban Environment," *2019 IEEE 90th Vehicular Technology Conference (VTC2019-Fall)*,2019, pp.1-5.
[10] N. Y. Mitsuishi *et al.*, "Propagation Model Analysis for 7- and 13-GHz Spectrum Sharing in Urban Environments"*IEEE Wireless Communications Letters*,2022, pp. 1965-1969.
[11] https://www.openstreetmap.org/#map=4/38.01/-95.84.
[12] Electronic Communication Committee (ECC), "Analysis of the suitability of the regulatory technical conditions for 5G MFCN operation in the 3400-3800 MHz band," Tec. Rep. June. 2018.
[13] ETSI, "5G; Study on channel model for frequencies from 0.5 to 100 GHz," 3GPP TR 38.901 version 14.0.0 Release 14.
[14] https://www.openstreetmap.org/map=4/38.01/-95.84.
[15] United States Census Bureau, [Online]. Available: https://www.census.gov/quickfacts/fact/table/blacksburgtownvirginia.